Supplementary Materials

Urinary extracellular vesicles detect altered renal circulation in human obesity

Mina Al-Saeedi[1,2,#], Lei Zhang[3,1,#], Aleksandar Denic[1], Kyra L Jordan[1], Fei Yuan[1,4], Xiangyang Zhu[1], Ailing Xue[1], Hui Tang[1], Alfonso Eirin[1], Amir Lerman[5,†], Mary Fidler[6], Andrew D. Rule[1], Aleksandra Kukla[1], Lilach O. Lerman[1]

[1]Division of Nephrology and Hypertension, Mayo Clinic, Rochester, MN 55905, USA. [2]Department of Medicine, Brookdale Hospital Medical Center, Brooklyn, NY 11212, USA. [3]Department of Urology, Zhongda Hospital, Southeast University, Nanjing 210009, Jiangsu, China.
[4]Department of Urology, Shanghai Children's Medical Center, affiliated to Shanghai Jiao Tong University School of Medicine, Shanghai 200127, China.
[5]Department of Cardiovascular Medicine, Mayo Clinic, Rochester, MN 55905, USA.
[6]Division of Anatomic Pathology, Mayo Clinic, Rochester, MN 55905, USA.
[#]These authors contributed equally to this work.
†Deceased.

Correspondence to: Dr. Lilach O. Lerman, Division of Nephrology and Hypertension, Mayo Clinic, Rochester, MN 55905, USA. E-mail: Lerman.Lilach@Mayo.Edu

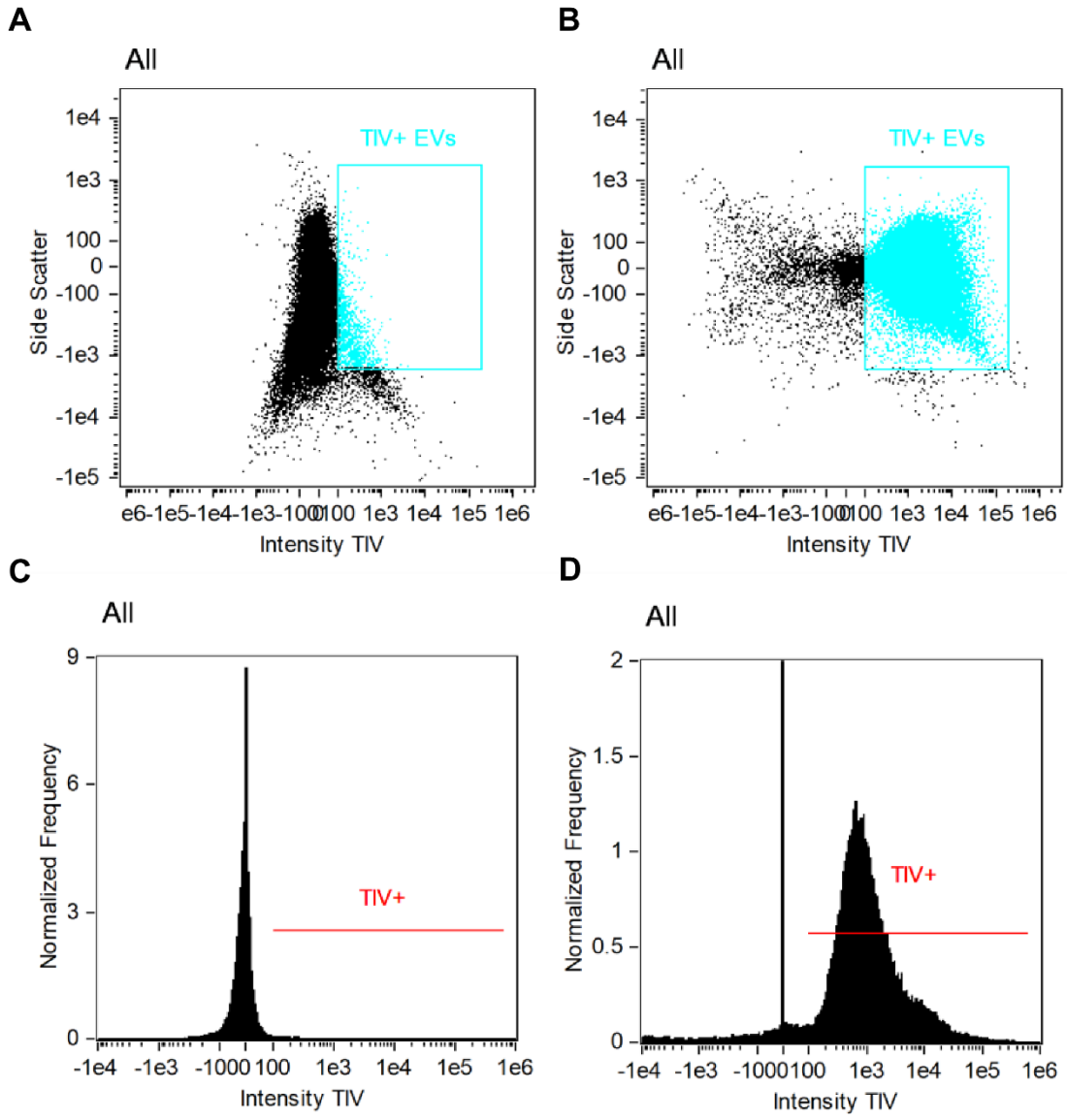

Figure S1. Validation of TIV⁺ gating strategy for urinary extracellular vesicles (uEVs). Side scatter (SSC) plots show uEVs stained without (A) or with (B) Tag-It Violet (TIV), illustrating the gating strategy. A TIV-negative control histogram (C) was used to define the fluorescence threshold for background exclusion, while the TIV-positive histogram (D) indicates the cutoff for positive event selection during flow cytometric analysis.

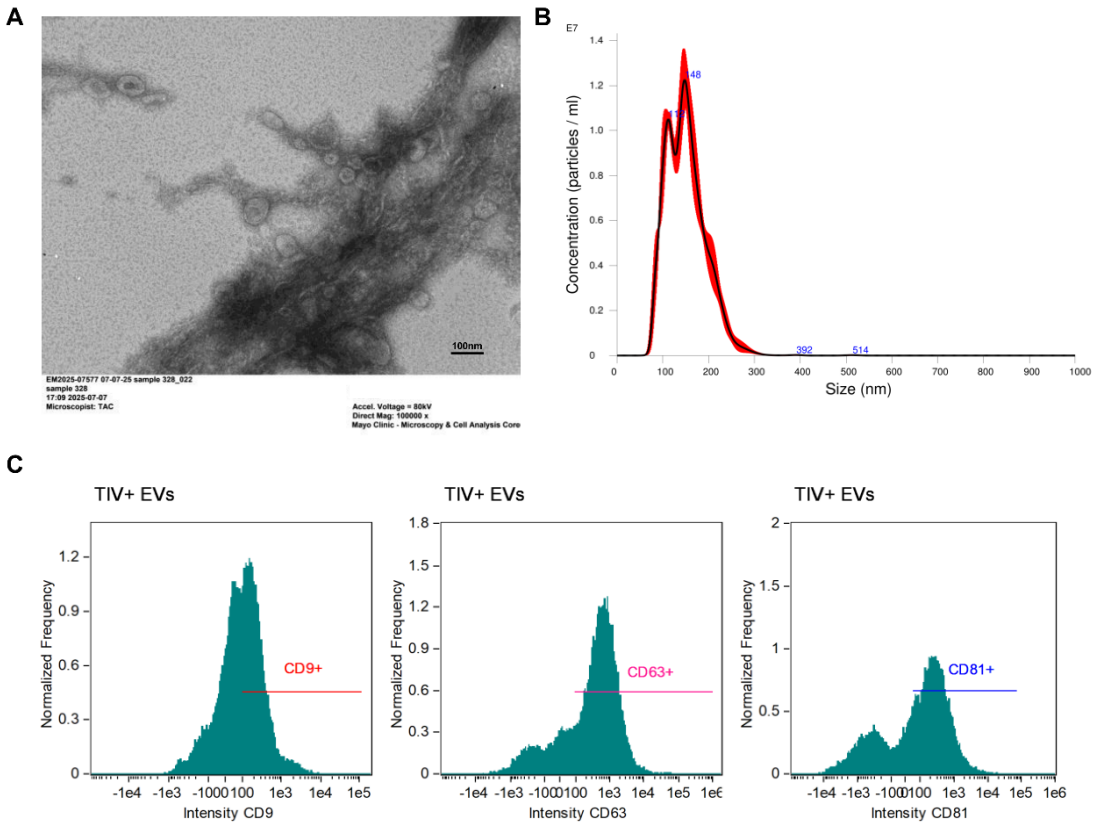

Figure S2. Characterization of uEVs. (A) Transmission electron microscopy (TEM) image showing typical round or cup-shaped morphology of urinary extracellular vesicles with diameters in the expected range (scale bar = 100 nm).(B) Nanoparticle tracking analysis (NTA) confirming the particle size distribution and concentration of isolated uEVs, with a predominant peak around 100~150 nm.(C) Flow cytometry analysis demonstrating the expression of canonical EV surface markers CD9, CD63, and CD81, confirming the enrichment of small EVs in urinary preparations. Representative histograms from independent samples are shown.

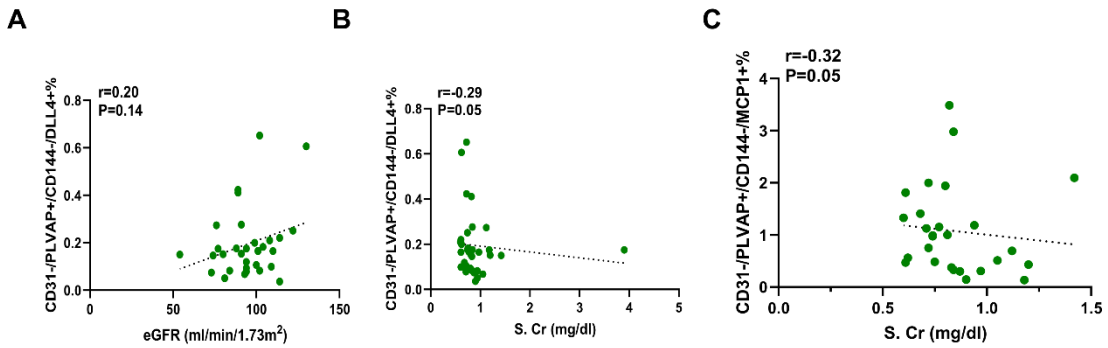

Figure S3. Correlations between PTC-derived uEV subsets and renal function. (A–B) $CD31^{-}/PLVAP^{+}/CD144^{-}/DLL4^{+}$ uEVs versus estimated glomerular filtration

rate (eGFR) and serum creatinine (S.cr). (C) $CD31^{-}/PLVAP^{+}/CD144^{-}/MCP\text{-}1^{+}$ uEVs versus S.cr. Spearman correlation coefficients (r) and p values are shown in each panel.

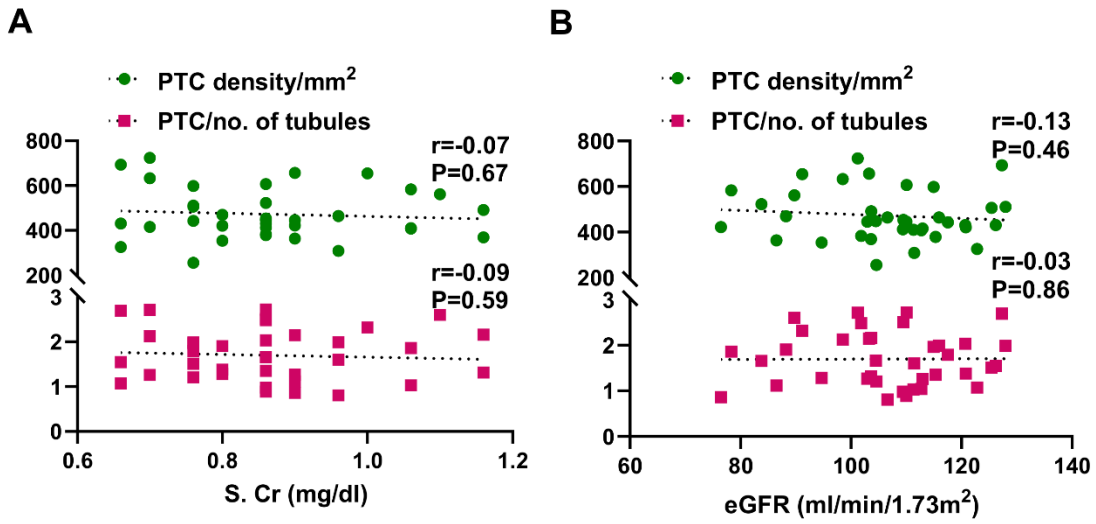

Figure S4. Correlations of PTC density and PTC-to-tubule ratio with kidney function. (A) Versus S.cr. (B) Versus eGFR. Spearman correlation coefficients (r) and p values are shown in each panel.